ANALYSIS OF ATOMISTIC/CONTINUUM COUPLING USING MESHLESS METHODS

M. Macri, P. W. Chung
U.S. Army Research Laboratory
Aberdeen Proving Ground, MD

ABSTRACT

In this paper, we compare three interpolation functions in a discretized continuum when used in coupled dynamic atomistic-to-continuum simulations. The focus is on assessing the ability of the discrete continuum model to capture and accurately represent transient effects, namely a travelling longitudinal wave, through both the mixed atomistic-continuum interface and the non-uniform continuum mesh beyond. We specifically examine the differences among Bubnov-Galerkin, partition of unity, and moving least squares finite element methods in the continuum part of the multiscale model. Our study shows that using partition of unity interpolation functions in the continuum produces superior results compared to the other two approaches.

INTRODUCTION

It is well known that continuum based techniques such as Lagrangian or Eulerian numerical methods, which use constitutive relations that do not account for the atomistic structure, are invalid beyond the scope of their calibration. In regions containing dislocations, mobile defects, or nonlinear material, these numerical methods have to be modified to capture important phenomena. Molecular dynamics (MD) is an excellent means for predicting interactions on an atomic scale as well as predicting the response when sub-micron scale phenomena occur. However, MD can be computationally expensive beyond small sample sizes and has difficulty implementing boundary conditions applied at a continuum scale. Therefore, to alleviate these problems multiscale methods have been developed in recent years to couple the continuum and atomistic scales together.

There has been extensive work on developing novel coupling techniques for linking atomistic and continuum scales. These techniques include the quasicontinuum method [1], bridging domain method [2], bridging scale method [3] and homogenization techniques [4,5], among others. A thorough review of several recent techniques is given in [6]. These techniques have been developed using the finite element method within the continuum scale. Though seemingly well known, to our knowledge, an examination of the level of approximation and choice of interpolation in the continuum region in and around the discrete atomistic domain has not been shown.

In this paper we show a comparative study of the quality of interpolation that best suits continuum methods in regions at and near the interface with a molecular dynamics region. We specifically examine interpolation functions prominent in general finite element methods and meshless methods – Bubnov-Galerkin, partition of unity [7], and moving least squares [8] – and assess their ability to capture a travelling wave through a discrete/continuum interface and a non-uniform finite element mesh (increasing element size away from the MD region). Within the interface region, where the continuum and atomistic scales overlap, the displacements on the continuum are dictated by the atomistic results generated from MD. In this study, the forces between the domains are communicated from the atoms to the continuum through ghost nodes.

CONTINUUM FORMULATION

We begin by reviewing the governing equations on the continuum scale. The conservation of momentum can be defined as:

$$\nabla_0\left(V_0\mathbf{P}\right)+\rho_0 V_0\mathbf{f}_0=\rho_0 V_0\ddot{\mathbf{u}} \tag{1}$$

where $\boldsymbol{P}$ is the first Piola-Kirchoff stress tensor, $\boldsymbol{f_0}$ is the body force, ρ_0 is the density, V_0 is the initial volume and $\ddot{\mathbf{u}}$ is the acceleration.

From classical hyperelastic continuum approximation we can define the first Piola-Kirchoff stress as:

$$\mathbf{P}=\frac{1}{V_0}\frac{\partial W}{\partial \mathbf{F}} \tag{2}$$

where W is the potential energy density, and $\boldsymbol{F}$ is the deformation gradient defined as:

$$\mathbf{F}=\frac{\partial \mathbf{x}}{\partial \mathbf{X}}=\frac{\partial \mathbf{u}}{\partial \mathbf{X}}+1 \tag{3}$$

where $\boldsymbol{X}$ denotes the reference configuration and $\boldsymbol{x}$ denotes the spatial or current configuration. In order to use equation (1) for numerical techniques such as general finite elements we use the principal of virtual work to obtain the variational form:

$$\int_{\Omega_0^C}\mathbf{w}\left[\nabla_0\left(V_0\mathbf{P}\right)+\rho_0 V_0\mathbf{f}_0-\rho_0 V_0\ddot{\mathbf{u}}\right]\partial\Omega_0^C=0 \tag{4}$$

where $\boldsymbol{w}$ is the virtual displacement. In the next two sections we define two different approaches to

Report Documentation Page

Form Approved
OMB No. 0704-0188

1. REPORT DATE	2. REPORT TYPE	3. DATES COVERED
DEC 2008	**N/A**	**-**

4. TITLE AND SUBTITLE	5a. CONTRACT NUMBER
Analysis Of Atomistic/Continuum Coupling Using Meshless Methods	5b. GRANT NUMBER
	5c. PROGRAM ELEMENT NUMBER
6. AUTHOR(S)	5d. PROJECT NUMBER
	5e. TASK NUMBER
	5f. WORK UNIT NUMBER
7. PERFORMING ORGANIZATION NAME(S) AND ADDRESS(ES) **U.S. Army Research Laboratory Aberdeen Proving Ground, MD**	8. PERFORMING ORGANIZATION REPORT NUMBER
9. SPONSORING/MONITORING AGENCY NAME(S) AND ADDRESS(ES)	10. SPONSOR/MONITOR'S ACRONYM(S)
	11. SPONSOR/MONITOR'S REPORT NUMBER(S)

12. DISTRIBUTION/AVAILABILITY STATEMENT
Approved for public release, distribution unlimited

13. SUPPLEMENTARY NOTES
See also ADM002187. Proceedings of the Army Science Conference (26th) Held in Orlando, Florida on 1-4 December 2008, The original document contains color images.

14. ABSTRACT

15. SUBJECT TERMS

16. SECURITY CLASSIFICATION OF:			17. LIMITATION OF ABSTRACT	18. NUMBER OF PAGES	19a. NAME OF RESPONSIBLE PERSON
a. REPORT	b. ABSTRACT	c. THIS PAGE			
unclassified	**unclassified**	**unclassified**	**UU**	**4**	

Standard Form 298 (Rev. 8-98)
Prescribed by ANSI Std Z39-18

approximating the displacement and virtual displacement, such that:

$$u(\mathbf{x}) = \sum_{I}^{N} h_I(\mathbf{x})\alpha_I \tag{5}$$

where $\boldsymbol{h}$ is a vector of interpolation functions and $\boldsymbol{\alpha}$ is a vector of coefficients.

PARTITION OF UNITY

For the partition of unity paradigm [6], define a weighting function, *W*, on each node that is compactly supported on $\overline{B}_I$ with the following properties:

1. $W_I(\mathbf{x}) \in C_0^s(\overline{B}_I)$ $\quad s \geq 0$
2. $W_I(\mathbf{x}) \geq 0$ $\quad \forall \mathbf{x} \in \overline{B}_I$
3. $W_I(\mathbf{x}) = 0$ $\quad$ *elsewhere*

The symbol $C_0^s(\overline{B}_I)$ stands for the space of functions that are compactly supported on $\overline{B}_I$, where in the case of general finite elements $\overline{B}_I$ is generated using neighboring elements, which have continuous derivatives of order *s*. We define the Shepard partition of unity function at each node *I* as:

$$\varphi_I^0(\mathbf{x}) = \frac{W_I(\mathbf{x})}{\sum_{J=1}^{N} W_J(\mathbf{x})} \tag{6}$$

From the partition of unity property it follows that the functions satisfy zeroth order consistency, i.e. they ensure that rigid body modes are exactly satisfied. The next step is to develop, at each node I, a local approximation space

$$V_I^{h,p} = span_{m\in\xi}\{p_m(\mathbf{x})\} \subset H^1(\overline{B}_I \cap \Omega) \tag{7}$$

where *h* is a measure of the size of the spheres, *p* is the polynomial order, ξ is an index set, H^1 is the first order Hilbert space, and $p_m(\mathbf{x})$ is a polynomial or other function. Finally, the global approximation space is defined by pasting together the local spaces as follows:

$$V^{h,p} = \sum_{I}^{N} \varphi_I^0 V_I^{h,p} \subset H^1(\Omega) \tag{8}$$

Hence, any function $v^{h,p} \in V^{h,p}$ can be written as:

$$v^{h,p}(\mathbf{x}) = \sum_{I=1}^{N} \sum_{m\in\xi} h_{\mathrm{Im}}(\mathbf{x})\alpha_{\mathrm{Im}} \tag{9}$$

$$h_{\mathrm{Im}}(\mathbf{x}) = \varphi_I^0(\mathbf{x}) p_m(\mathbf{x}) \tag{10}$$

and h_{Im} is the shape function at node *I* corresponding to the m[th] degree of freedom.

MOVING LEAST SQUARES

In moving least squares we set the approximation to:

$$v^{h,p}(\mathbf{x}) = \sum_{m=1}^{\xi} p_m(\mathbf{x})\beta_m(\mathbf{x}) = \mathbf{p}^T(\mathbf{x})\boldsymbol{\beta}(\mathbf{x}) \tag{11}$$

where $\boldsymbol{p}$ is a vector composed of the monomial basis functions as in equation (7) and $\boldsymbol{\beta(x)}$ is a vector composed of their coefficients. These coefficients are obtained by using a weighted least square fit for the local approximation. We can derive this by minimizing the difference between the local approximation and the function, such that:

$$\frac{\partial J}{\partial \boldsymbol{\beta}} = \mathbf{A}(\mathbf{x})\boldsymbol{\beta}(\mathbf{x}) - \mathbf{B}(\mathbf{x})\boldsymbol{\alpha} = 0 \tag{12}$$

$$\mathbf{A}(\mathbf{x}) = \mathbf{P}^T \boldsymbol{\Psi}(\mathbf{x})\mathbf{P} \tag{13}$$

$$\mathbf{B}(\mathbf{x}) = \mathbf{P}^T \boldsymbol{\Psi}(\mathbf{x}) \tag{14}$$

where $\boldsymbol{P}$ is a matrix composed of the monomial basis functions and $\boldsymbol{\psi}$ is a matrix composed of the weighting functions having the same properties as those used in partition of unity interpolation functions. This results in:

$$v^{h,p}(\mathbf{x}) = \mathbf{p}^T(\mathbf{x})\mathbf{A}^{-1}(\mathbf{x})\mathbf{B}(\mathbf{x})\boldsymbol{\alpha} = \sum_{I}^{N} h_I(\mathbf{x})\alpha_I \tag{15}$$

And the shape function is defined as:

$$h_I(\mathbf{x}) = \mathbf{p}^T(x)\mathbf{A}^{-1}(\mathbf{x})\mathbf{p}(\mathbf{x}_I)W_I(\mathbf{x}) \tag{16}$$

MOLECULAR DYNAMICS

For the atomistic scale the governing equation for MD is Newton's equation of motion defined as

$$m_a \ddot{\mathbf{u}}_a = f_a \tag{17}$$

where m_a is the mass, $\ddot{\mathbf{u}}_a$ is the acceleration and $\boldsymbol{f_a}$ is the force acting on discrete atoms, *a*. For our study we will only examine short range interactions. The force is defined as:

$$f_a = -\sum_{b\neq a}^{N^M} \frac{\partial \phi_{ab}}{\partial \mathbf{x}_a} \tag{18}$$

where ϕ_{ab} is the interatomic potential.

In this paper we specifically examine a linear harmonic potential and a non-linear Lennard-Jones potential, where the harmonic potential is given as:

$$\phi_{ab}^H = \frac{1}{2}k(r_{ab} - r_{ab,0})^2 \tag{19}$$

where k is a constant and r_0 is the zero potential distance between two atoms. The Lennard-Jones potential is defined as:

$$\phi_{ab}^{LJ} = 4\varepsilon\left[\left(\frac{\sigma}{r_{ab}}\right)^{12} - \left(\frac{\sigma}{r_{ab}}\right)^{6}\right] \tag{20}$$

where ε and σ and constants.

COUPLING

In figure 1 we define the domain as discretized into a region in which the continuum equations are applied, Ω^C, and a region in which MD is applied, Ω^A. There is an overlap between these two regions defined as the interface region Ω^I.

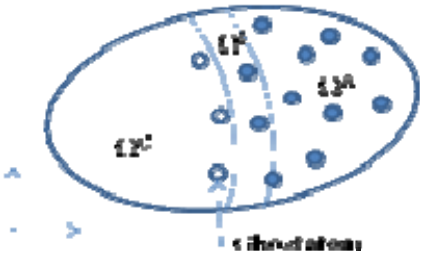

Figure 1: Coupling Domain

The constraint that matches atoms to nodes in the interface is applied through a penalty formulation. The result is a modified variational form of (4):

$$\left(\frac{1}{\Delta t^2}\mathbf{M} + \sum_{i=1}^{N^I}\gamma\left(\mathbf{h}\left(\mathbf{X}_i^A\right)^T\mathbf{h}\left(\mathbf{X}_i^A\right)\right)\right)^{t+\Delta t}\boldsymbol{\alpha} = \mathbf{f}_{ext} - \mathbf{f}_{\text{int}} + \left(\frac{1}{\Delta t^2}\mathbf{M}\right)\left(2^t\boldsymbol{\alpha} - {}^{t-\Delta t}\boldsymbol{\alpha}\right) + \sum_{i=1}^{N^I}\gamma\left(\mathbf{h}\left(\mathbf{X}_i^A\right)^T\mathbf{u}_i^A\right) \tag{21}$$

Where is the penalty constant which is generally a large positive number. To enforce the interface conditions for MD, ghost atoms are placed in the continuum region (see figure 1) to avoid a surface layer or unphysical termination in the interface.

NUMERICAL EXAMPLES

We present three examples of a Gaussian wave propagating through atomic medium to illustrate the preliminary results. The first two examples are demonstrated in a 1D domain, while the third is example is in two dimensions.

For the first two examples the analysis is preformed on a 1D section of atoms and compared with simulation performed using MD throughout the entire model using 79 atoms. For the comparative study, the domain is discretized such that for $-2 \le x \le 2$ each atom is individually resolved and from $-10 \le x \le 2$ and $2 \le x \le 10$ the different numerical interpolation schemes are applied. We compare the use of Bubnov-Galerkin, finite elements, partition of unity and moving least squares interpolation functions to full MD throughout the domain. The initial wave function is shown in figure 2.

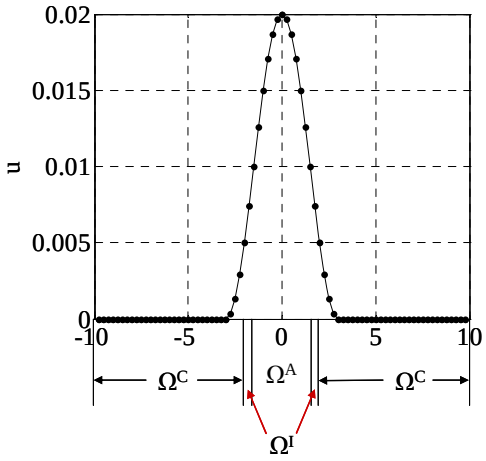

Figure 2: 1D Example formulation

For the first example we use a harmonic interatomic potential. The results of the error in the displacements as the wave propagates are shown in figure 3. The red line represents the error in a continuum disctretized using finite elements the green line represents moving least squares functions and the blue represents partition of unity functions.

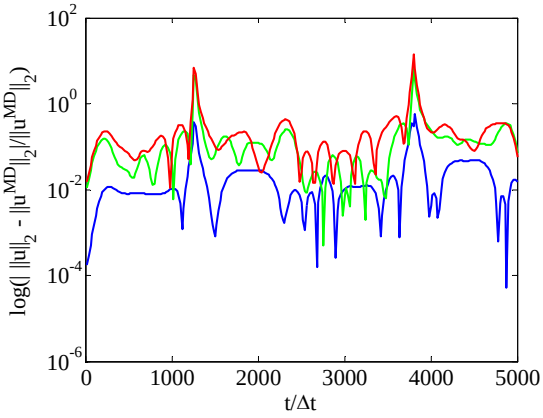

Figure 3: Error comparisons for Harmonic potential.

From this result, the partition of unity interpolation scheme is perform extremely well when compared to the full-MD analysis. Whereas finite elements and MLS functions perform about the same. Spikes in the error

occur for wall three techniques when the wave passes through the boundaries.

For the second example we compare the analysis shown in figure 2 using a Lennard-Jones potential. The results are shown in figure 4. The results colaberate the above example with partition of unity functions performing better then the other two techniques.

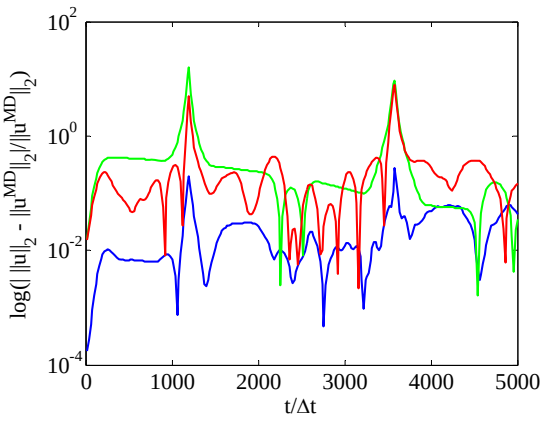

Figure 4: Error comparisons for Lennard-Jones potential

For the 2D example the domain is discretized such that for $-2 \le x, y \le 2$ each atom is individually resolved and from $-10 \le x, y \le 2$ and $2 \le x, y \le 10$ the different numerical interpolation schemes are applied. We compare the use of Bubnov-Galerkin, finite elements and partition of unity interpolation functions to full MD throughout the domain. We use a harmonic interatomic potential in this example. The initial wave function is shown in figure 5.

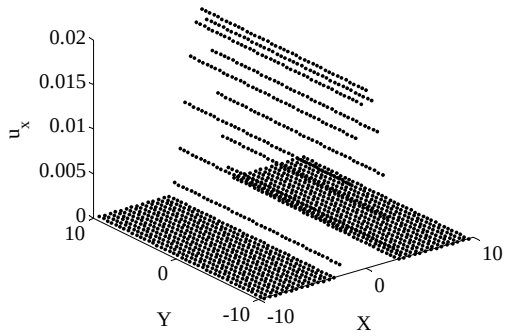

Figure 5: 2D example formulation

The results, shown in figure 6, demonstrate again that partition of unity shape function out perform finite elements, however, the margin is much less.

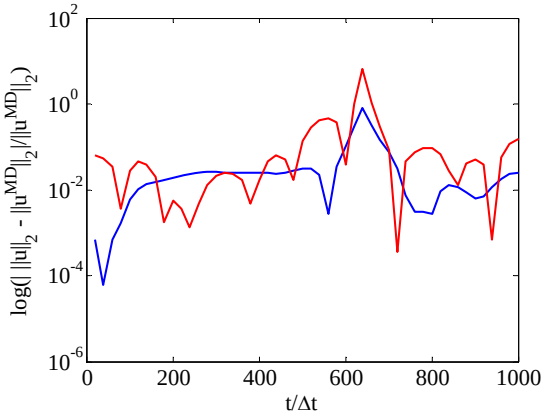

Figure 3: Error comparisons for 2D example.

ACKNOWLEDGEMENTS

The authors gratefully acknowledge the U.S. Army Research Laboratory for support through the National Research Council Resident Research Associateship Program and the U.S. Army Major Shared Resource Center for computing support and resources.

REFERENCE

1. Tadmor, E.B., Ortiz, M., Phillips, R., (1996) *Phil. Mag.*, A73, 1529.
2. Zhang, S., Khare, R., Lu, Q. and Belytschko, T. (2007) *Int. J. Numer. Meth. Engng*, Vol. 70, pp. 913–933.
3. Tang, S., Hou, T.Y. and Liu, W.K. (2006) *Int. J. Numer. Meth. Engng*, Vol. 65, pp. 1688–1713.
4. Fish, J., Chen, W. and Li, R. (2007) *Comput. Methods Appl. Mech. Engrg.*, Vol. 196, pp. 908–922.
5. Chung, P. and Namburu, R. (2003) *International Journal of Solids and Structures*, Vol. 40, pp. 2563–2588.
6. Curtin, W.A. and Miller, R. (2003) *Modelling Simul. Mater. Sci. Eng.*, Vol. 11, pp. R33–R68.
7. Melenk, J.M. and Namburu, I. (1996) *Comp Methds in App Mech and Engg*, Vol. 139, pp. 289–314.
8. Belytschko, T., Lu, Y.Y. and Gu, L. (1994) *Int. J. Numer. Meth. Engng*, Vol. 37, pp. 229–256.